Can inertial electrostatic confinement work beyond the ion–ion collisional time scale?

W. M. Nevins
Lawrence Livermore National Laboratory, Livermore, California 94550

(Received 20 March 1995; accepted 6 July 1995)

Inertial electrostatic confinement (IEC) systems are predicated on a nonequilibrium ion distribution function. Coulomb collisions between ions cause this distribution to relax to a Maxwellian on the ion–ion collisional time scale. The power required to prevent this relaxation and maintain the IEC configuration for times beyond the ion–ion collisional time scale is shown to be greater than the fusion power produced. It is concluded that IEC systems show little promise as a basis for the development of commercial electric power plants. © *1995 American Institute of Physics.*

I. INTRODUCTION

Inertial electrostatic confinement (IEC) is a concept from the early days of fusion research. Work on magnetic confinement fusion in the Soviet Union was begun by Sakharov and others in response to a suggestion from Lavrent'ev that controlled fusion of deuterium could be achieved in an IEC device.[1] The concept was independently invented in the United States by Farnsworth.[2] Inertial electrostatic confinement schemes require the formation of a spherical potential well. Low-energy ions are injected at the edge and allowed to fall into this potential well. If the ion injection energy is low, the ions have a low transverse energy, low angular momentum, and must pass near the center of the spherical potential well on each transit. The repeated focusing of the ions at the center of the well results in peaking of the fuel density and greatly enhances the fusion rate relative to what would be achieved in a uniform plasma of the same volume and stored energy. This strong ion focusing at the center of the potential well is the defining feature of IEC schemes. The plasma configuration envisioned by proponents of IEC fusion systems is illustrated in Fig. 1.

Early spherical electrostatic traps[2–4] required grids to produce the confining potential. Calculations of grid cooling requirements[5] indicated that this concept would require a grid radius greater than 10 m to achieve net energy output, leading to an impractical reactor. It was suggested that the concept could be improved by using a magnetic field to shield the grid from the hot plasma; and in the Soviet Union the concept evolved into an investigation of electrostatically plugged cusps (see Ref. 6 for an excellent review of this field). In this evolution from a purely electrostatic confinement scheme into a magnetoelectrostatic-confinement scheme it appeared that a key advantage had been lost—the confining magnetic field lacks spherical symmetry so the strong ion focus is lost within a few ion transit times because the angular momentum of the ions is not conserved in the absence of spherical symmetry.

Recently, there has been a resurgence of interest in electrostatic confinement fusion. Two new concepts for forming the spherical potential well that do not involve internal grids have been proposed—the Polywell™ and the Penning trap. In a Penning trap a spherical effective potential well is formed in a rotating frame by a combination of electrostatic and magnetic fields.[7] In the Polywell™ configuration,[8–10] a polyhedral magnetic cusp is used to confine energetic electrons. The space charge of these magnetically confined electrons then creates a potential well to confine the ions.

In estimating the importance of collisional effects on an IEC fusion reactor, we will use the parameters in Table I. These parameters generally follow those suggested by Bussard[9] and Krall.[10] We have adjusted the operating point somewhat to take account of our more accurate calculation of the fusion reactivity (see Sec. III) and to ensure that the projected operating point is consistent with the model described in Sec. II. We assume a deuterium–tritium (DT) fueled IEC reactor because the power balance is most favorable with this fuel, and we find power balance to be the critical problem.

In this work a perfectly spherical potential is assumed, thus assuring that the ion focus can be maintained over many ion transit times (about 1 μs for the IEC reactor parameters of Table I). Ion–ion collisions act on a substantially longer time scale. The ion focusing that defines IEC systems is associated with a strong anisotropy in the ion distribution function. Ion–ion collisions tend to reduce this anisotropy on the ion–ion collisional time scale (about 1 s for the IEC reactor parameters of Table I). It is possible to maintain this nonequilibrium ion distribution function with sufficient recirculating power. The object of this paper is to compute the collisional relaxation rates and estimate the recirculating power required to maintain an IEC reactor beyond the ion–ion collisional time scale.

Proponents of IEC systems often assume an ion distribution function that is nearly monoenergetic.[2,9–11] There is not a necessary connection between maintaining the ion focus (which results from the dependence of the ion distribution function on angular momentum) and the variation of the ion distribution function with energy. However, some proponents (see especially Ref. 9) believe this to be a second key feature of IEC systems because of the substantial increase in the fusion rate coefficient for a monoenergetic distribution relative to that of a thermal ion distribution (but see Sec. III, where it is shown that this increase is not significant).

Our approach in analyzing IEC systems is to develop a simple model that contains the essential features described by proponents of IEC systems (electrostatic confinement, strong ion focusing, and a monoenergetic ion distribution

 1070-664X/95/2(10)/3804/16/$6.00

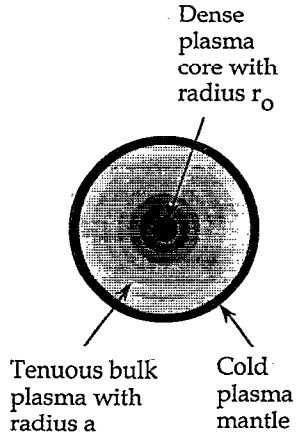

FIG. 1. The IEC plasma is divided into three regions: a dense plasma core, a bulk plasma where the density falls approximately as $1/r^2$, and a cold plasma mantle where the ions are reflected from the edge of the potential well and the mean ion kinetic energy is low.

function); and then to use this model as a basis for the calculation of collisional relaxation rates, estimates of the fusion power produced by the systems, and the auxiliary power required to maintain the nonequilibrium IEC configuration. A successful IEC device must maintain a high convergence ratio, a/r_0. We find this to be a useful ordering parameter, and use it freely to identify leading terms in the collisional relaxation rates and power balance.

In Sec. II we present a model IEC ion distribution function and show that it reproduces the central features envisioned by proponents of IEC systems. In Sec. III we compute the averaged fusion rate coefficient for this distribution and show that it is not substantially greater than that for a Maxwellian distribution with similar mean energy per particle. In Sec. IV we compute the collisional rate of increase in the angular momentum squared $\langle L^2\rangle$ (which determines the rate of decay of the ion focus), and the collisional rate of increase in the energy spread of the ion distribution resulting from collisions in the plasma bulk and core between ions with large relative velocities. In Sec. V we compute the collisional rates of change in $\langle L^2\rangle$ and energy spread due to collisions in the plasma bulk between ions with small relative velocities. Assuming that the ion distribution is initially strongly focused and nearly monoenergetic, this analysis indicates that the instantaneous rate of relaxation toward a Maxwellian is $(a/r_0)\nu_{ii}$, where r_0 is the radius of the ion focus, a is the radius of the bulk plasma, and ν_{ii} is the ion–ion collision frequency evaluated at the volume-averaged density. The ion focus degrades progressively, so that it takes a time of order ν_{ii}^{-1} to complete the relaxation to an isotropic Maxwellian. Clearly, some intervention is required if the nonthermal ion distribution is to be maintained beyond the ion collisional time scale. In Sec. VI we analyze two schemes proposed by proponents of IEC systems,[9,11] and conclude that they will not be effective in maintaining the nonthermal ion distribution function. In Sec. VII we examine schemes for maintaining nonthermal ion distributions that rely on controlling the lifetime of ions in the electrostatic trap. We find that these schemes require the recirculating power be greater than the fusion power. We conclude that IEC devices show little promise as a means for generating electric power. However, they may be useful as a means of generating 14 MeV neutrons for other applications.

TABLE I. Reference IEC reactor parameters.

Quantity	Symbol	Value
Potential well depth	ϕ_0	50.7 keV
Plasma radius	a	1 m
Core radius	r_0	1 cm
Volume-averaged density	$\langle n_i\rangle$	0.5×10^{20} m^{-3}
Peak ion density	n_{i0}	3.3×10^{23} m^{-3}
Fusion power	P_{fusion}	590 MW

II. THE MODEL

Two constants of the single-particle motion for an ion of species "s" in a spherically symmetric trap are the total energy,

$$\epsilon \equiv 1/2 m_s v^2 + q_s\phi(r); \tag{1}$$

and the square of the particle's angular momentum,

$$L^2 \equiv (m_s \mathbf{v}\times\mathbf{r})^2. \tag{2}$$

We consider weakly collisional systems, in which the collision frequency (ν) and fusion rate ($n_s\langle\sigma v\rangle_{\text{DT}}$) are small compared to the transit frequency (ω_b) in the electrostatic well. At leading order in ν/ω_b, the ion distribution function is then a function of the single-particle constants of motion. We assume an ion distribution function of the form

$$f_s = f_s(\epsilon, L^2). \tag{3}$$

The particle density at radius r is then given by

$$n_s(r) = \pi \int d\epsilon\, dL^2 \frac{\partial(v_r, v_\perp^2)}{\partial(\epsilon, L^2)} f_s(\epsilon, L^2), \tag{4}$$

where the Jacobian between velocity space and (ϵ, L^2) space is

$$\pi \frac{\partial(v_r, v_\perp^2)}{\partial(\epsilon, L^2)} = \frac{\pi}{m_s^3 r^2 v_r} \tag{5}$$

and

$$v_r(\epsilon, L^2) = \sqrt{\frac{2}{m_s}(\epsilon - q_s\phi) - \frac{L^2}{m_s^2 r^2}}. \tag{6}$$

We consider ion distributions that are nearly monoenergetic and strongly focused at the center of the sphere (i.e., distributions with low angular momentum). An ion distribution function with these properties is

$$f_s(\epsilon, L^2) = C_s \delta(\epsilon) H(L_0^2 - L^2), \tag{7}$$

where C_s is a constant (to be evaluated below) and $H(x)$ is a Heaviside function.

In our calculations we consider a "square-well" potential,

$$\phi(r)=\begin{cases}-\phi_0, & r<a,\\ +\phi_0, & r\geq a.\end{cases}$$

A substantial confining potential ($+\phi_0$) is assumed in order to ensure that the dominant collisional effect is thermalization of the ion distribution, rather than ion upscatter (in energy) followed by loss from the potential well. The ion number density corresponding to our model distribution function is

$$n_s(r)=\int_0^\infty dL^2\int_{-q_s\phi_0+L^2/2m_sr^2}^{q_s\phi_0+L^2/2m_sa^2}d\epsilon\,\frac{\pi}{m_s^3r^2v_r}\times C_s\delta(\epsilon)H(L_0^2-L^2), \tag{8}$$

$$=n_{s0}\times\begin{cases}1, & r<r_0,\\ \dfrac{r_0^2/r^2}{1+\sqrt{1-r_0^2/r^2}}, & r>r_0,\end{cases} \tag{9}$$

where $n_{s0}\equiv 2\pi v_s C_s/m_s$, $v_s\equiv\sqrt{2q_s\phi_0/m_s}$, $L_r\equiv mv_sr$, and $r_0\equiv L_0/m_sv_s$.

We evaluate the constant C_s by noting that the total number of ions in the trap, N_s, is given by

$$N_s=\int_0^\infty 4\pi r^2\,dr\,n_s(r)$$

$$=\frac{4\pi a^3}{3}n_{s0}[1-(1-r_0^2/a^2)^{3/2}] \tag{10}$$

$$\approx 2\pi r_0^2 a n_{s0}\quad (r_0\ll a). \tag{11}$$

Hence, the central ion density, n_{s0}, is

$$n_{s0}\approx\frac{N_s}{2\pi r_0^2 a}\approx\frac{2}{3}\left(\frac{a}{r_0}\right)^2\langle n_s\rangle_{\rm Vol}, \tag{12}$$

where $\langle n_s\rangle_{\rm Vol}\equiv N_s/V$ is the volume-averaged density, and $V=4\pi/3a^3$ is the volume of the trap. The corresponding value of C_s is

$$C_s\approx\frac{m_sN_s}{4\pi^2r_0^2av_s}. \tag{13}$$

Restricting the ion distribution function to low values of angular momentum, $|L|\leq L_0=m_sv_sr_0$, has the effect of increasing the central ion density relative to what it would be for an isotropic ion velocity distribution by the factor $0.67(a/r_0)^2$. We conclude that the model IEC ion distribution function of Eq. (7) reproduces the essential features of inertial electrostatic confinement schemes—electrostatic confinement, strong central peaking of the fuel ion density, and a monoenergetic energy distribution.

III. FUSION POWER GENERATION

For a deuterium–tritium plasma, the total fusion power is given by

$$P_{\rm fusion}=Y_{\rm DT}\int d^3r\,n_d(r)n_t(r)\langle\sigma v\rangle_{\rm DT}(r), \tag{14}$$

where $Y_{\rm DT}=17.6$ MeV is the fusion yield per event. We assume an equal mixture of deuterium and tritium (with no impurities), and that deuterium and tritium distribution functions have the same convergence ratio, so that

$$n_i(r)=n_d(r)+n_t(r)=2n_d(r)=2n_t(r). \tag{15}$$

If the fusion rate coefficient, $\langle\sigma v\rangle_{\rm DT}$, were independent of radius, then the fusion power would be given by

$$P_{\rm fusion}=\frac{1}{4}Y_{\rm DT}\langle\sigma v\rangle_{\rm DT}\int d^3r\,n_i^2(r)$$

$$\approx\frac{2\pi}{3}r_0^3n_{i0}^2Y_{\rm DT}\langle\sigma v\rangle_{\rm DT}\left(1-\frac{3}{8}\frac{r_0}{a}+\cdots\right), \tag{16}$$

where we have used the fact that, for the model distribution described in Sec. II,

$$\int d^3r\,n_i^2(r)\approx\frac{4\pi}{3}r_0^3n_{i0}^2\left(2-\frac{3}{4}\frac{r_0}{a}+\cdots\right). \tag{17}$$

This motivates the definition

$$\langle\sigma v\rangle_{\rm DT}^{\rm eff}\equiv\frac{P_{\rm fusion}}{\frac{1}{4}Y_{\rm DT}\int d^3r\,n_i^2(r)}. \tag{18}$$

The radial dependence of the fusion rate coefficient arises because, even for monoenergetic distributions, the fusion rate has to be averaged over the angle between the colliding particles. This angular distribution varies as a function of radius. For the model described in Sec. II the angular distribution function $g(\mu)$ is isotropic within the core (i.e., for $r\leq r_0$), while outside of the core ($r>r_0$) the angular distribution [normalized such that $\int g(\mu)d\mu\equiv 1$] satisfies

$$g(\mu)=\begin{cases}\dfrac{1}{2\sqrt{1-r_0^2/r^2}}, & |\mu|>\sqrt{1-r_0^2/r^2},\\ 0, & |\mu|<\sqrt{1-r_0^2/r^2},\end{cases} \tag{19}$$

where μ is the cosine of the angle between the ion velocity and the unit vector in the radial direction, $\hat{\mathbf{e}}_{\rm r}$.

The averaged fusion rate coefficient for an ion with zero angular momentum (i.e., an ion for which $\mu=\pm 1$) colliding with background ions described by the model IEC distribution is

$$\langle\sigma v\rangle_{\rm DT}=\int_{-1}^{1}d\mu\,g(\mu)\sigma(E_{\rm cm})v_r(\mu), \tag{20}$$

where the relative velocity v_r satisfies

$$v_r^2(\mu)=v_d^2-2\mu v_dv_t+v_t^2, \tag{21}$$

the center-of-mass energy is given by $E_{\rm cm}=\frac{1}{2}m_rv_r^2$, and the reduced mass by

$$m_r=\frac{m_dm_t}{m_d+m_t}, \tag{22}$$

while the subscripts "d" and "t" label the ion species, deuterium and tritium.

We have evaluated the μ integral numerically using an analytic fit to the center-of-mass fusion cross sections developed by Bosch and Hale[12] (which is accurate to within 2% over the relevant energy range). We find significant variation in $\langle\sigma v\rangle_{\rm DT}$ with both radius and potential well depth. The rate

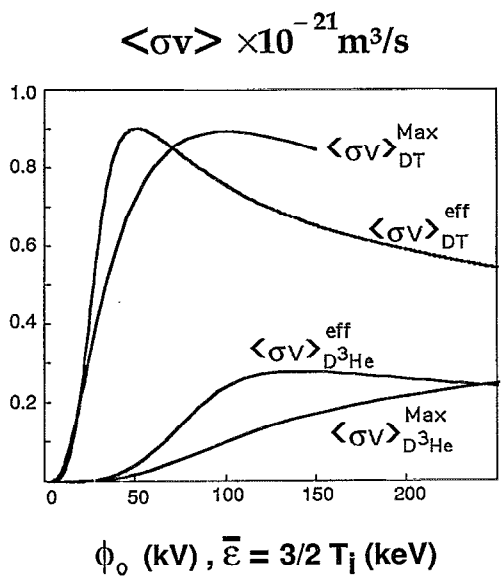

FIG. 2. Effective fusion rate coefficient for DT and D^3He reactions versus the potential well depth, ϕ_0. The kinetic energy of each particle is $q\phi_0$. The corresponding Maxwellian-averaged rate coefficients, plotted against the mean ion energy, $\bar{\epsilon}=\frac{3}{2}T$, are shown for comparison.

coefficient in the core ($r \leq r_0$) is that of an isotropic, monoenergetic distribution, as previously evaluated in this context by Miley *et al.*[13] and Santarius *et al.*[14] In the bulk region ($r_0<r<a$), the rate coefficient rapidly approaches that of two counterstreaming beams, as considered by Bussard.[9]

In evaluating the total fusion power, one should integrate over the angular distributions of both incident ions. The rate coefficient of Eq. (20) is averaged only over the angular distribution of one of the incident ions. However, it reproduces the correct result for $r \leq r_0$ (where both ion distributions are isotropic), and for $r \gtrsim 2r_0$, where the dominant contribution to the rate coefficient comes from counterstreaming ions. Hence, only a small error is introduced by replacing this second angular average with its value for $L^2=0$. Using this approximation, we have evaluated the effective rate coefficient, as defined in Eq. (18) as a function of the potential well depth for both DT and D–^{3}He reactions. These results are displayed in Fig. 2, together with corresponding Maxwellian-averaged rate coefficients.

In computing the effective rate coefficients, $\langle \sigma v \rangle_{ss'}^{\text{eff}}$, displayed in Fig. 2, we have assumed that the kinetic energy of the incident ions "s" and "s'" are given by $q_s\phi_0$ and $q_{s'}\phi_0$, respectively, because we find no advantage in choosing the energy of the heavier ion to be smaller than that of the lighter ion by the ion mass ratio (an ordering of the ion energies was recommended in Ref. 10 as a means of minimizing the energy diffusion resulting from collisions in the "bulk" region, $r_0<r<a$). This issue is discussed further in Sec. IV.

The Maxwellian-averaged fusion rate coefficients displayed in Fig. 2 were computed following Bosch and Hale.[12] The monoenergetic IEC rate coefficient $\langle \sigma v \rangle_{\text{DT}}^{\text{eff}}$ has a peak value of 0.90×10^{-21} m^3/s at a potential well depth $\phi_0=50.7$ kV; while the Maxwellian-averaged fusion rate coefficient $\langle \sigma v \rangle_{\text{DT}}^{\text{Max}}$ has a peak value of 0.89×10^{-21} m^3/s at a mean ion energy $\bar{\epsilon}=113$ keV (or $T_i=75$ keV). The monoenergetic IEC rate coefficient for D^3He, $\langle \sigma v \rangle_{\text{D}^3\text{He}}^{\text{eff}}$ has a peak value of 2.8×10^{-22} m^3/s at $\phi_0=140$ kV. Miley[15] reports a maximum value in the Maxwellian-averaged D^3He rate coefficient, $\langle \sigma v \rangle_{\text{D}^3\text{He}}^{\text{Max}}=2.5\times10^{-22}$ m^3/s at a mean ion energy $\bar{\epsilon}=375$ keV (or $T_i=250$ keV). The somewhat larger difference (about 11%) between the peak in these averaged rate coefficients is similar in magnitude to the change in the D^3He rate coefficient associated with the improved parametrization of the fusion cross section developed by Bosch and Hale (see Fig. 22 of Ref. 13). We see that, despite claims to the contrary,[9] the averaged rate coefficient for a monoenergetic IEC system is not significantly greater than the Maxwellian-averaged fusion rate coefficient at similar mean ion energies.

We conclude that significant increases in the power density of an IEC system relative to other confinement systems result from the choice of a higher mean ion energy at the projected operating point and from the strong central peaking of the ion density associated with the anisotropic ion distribution function assumed by proponents of IEC systems.

IV. COLLISIONAL RELAXATION OF THE ION DISTRIBUTION FUNCTION

The strong focusing of ions at the center of the well is the defining feature of IEC systems. This focusing leads to a substantial enhancement of the total fusion power at fixed stored energy. The total fusion power within our square-well model,

$$P_{\text{fusion}}=\frac{1}{4}Y_{\text{DT}}\int d^3r\, n_i^2(r)\langle \sigma v \rangle_{\text{DT}}(r) \approx \frac{8}{9}\frac{a}{r_0}\left(\frac{\langle n_i \rangle_{\text{Vol}}}{2}\right)^2 VY_{\text{DT}}\langle \sigma v \rangle_{\text{DT}}^{\text{eff}}, \tag{23}$$

is enhanced relative to what would be obtained with an isotropic ion distribution function (for which $n_i=\langle n_i \rangle_{\text{Vol}}$) by the factor $(8/9)a/r_0$. This enhancement results from the central peaking of the ion density, which, in turn, depends critically on maintaining a strong anisotropy in the ion distribution function [i.e., ensuring that $f_s(\epsilon,L^2)$ goes to zero rapidly for $L^2>(m_s v_s r_0)^2$]. Hence, it is important to examine effects that will tend to reduce this anisotropy in the ion distribution function.

Ion–ion collisions are an obvious mechanism for reducing the ion anisotropy. It follows from the Boltzmann H theorem that ion–ion collisions will drive the system to an equilibrium in which $f_s(\epsilon,L^2)\sim\exp(-\epsilon/T)$. That is, to a state in which there is no ion anisotropy, and the only variation in the ion density arises from variations in the potential, such that $n_s(r)\sim\exp[-q_s\phi(r)/T]$. If the ion distribution function is allowed to relax to thermal equilibrium the key advantage of IEC systems (enhanced fusion power at fixed stored energy due to strong density peaking) is lost. However, ion collision rates are low (of the order of 1 Hz) at the energy and densities projected for IEC reactors. Hence, the power required to maintain a nonequilibrium ion distribution function might be less than the fusion power produced. In order

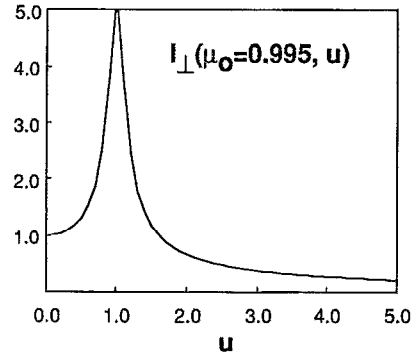

FIG. 3. Here $I_\perp(\mu_0,u)$ is displayed as a function of test particle speed (u) for $\mu_0=0.995$ (corresponding to $r=10r_0$). The resonance at $u=1$ results from self-collisions among comoving particles.

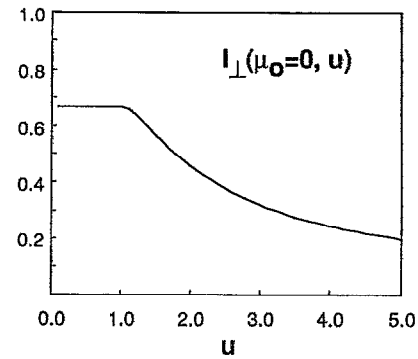

FIG. 4. Here $I_\perp(\mu_0,u)$ is displayed as a function of test particle speed for $\mu_0=0$, corresponding to radial locations in the plasma core, $r\leq r_0$.

to investigate this possibility we evaluate the collisional relaxation rates of the ion distribution function.

A. Collisional relaxation of ion anisotropy

Coulomb collisions will result in an increase in $\langle L^2\rangle$ due to transverse scattering (that is, scattering of the ion velocity, so that it has a component in the plane perpendicular to $\hat{\mathbf{e}}_r$). In Appendix A we show that, in the limit $L^2\to 0$ (so that the ion velocity is nearly radial over most of its orbit), the collisional rate of increase in the mean-square transverse velocity for ions of species s and speed

$$v_s\equiv\sqrt{\frac{2q_s\phi_0}{m_s}} \tag{24}$$

is given by

$$\frac{d}{dt}\langle\Delta v_\perp^2\rangle=2v_s^2\sum_{s'}\nu_0^{s/s'}u_{s'}I_\perp(\mu_0,u_{s'}), \tag{25}$$

where

$$u_{s'}\equiv\frac{v_s}{v_{s'}} \tag{26}$$

following Book,[16] we have defined

$$\nu_0^{s/s'}\equiv\frac{4\pi q_s^2q_{s'}^2n_{s'}\mathrm{Ln}\Lambda_{ss'}}{m_s^2v_s^3} \tag{27}$$

and

$$\mu_0=\begin{cases}0, & r\leq r_0,\\ \sqrt{1-r_0^2/r^2}, & r>r_0,\end{cases} \tag{28}$$

is the cosine of the angle between $\mathbf{v}$ and $\hat{\mathbf{e}}_r$ at which the model IEC distribution function goes to zero for the given radius.

The variation of the collision integral $I_\perp(\mu_0,u)$ with particle speed is shown in Fig. 3 for a typical location in the plasma bulk, $r=10r_0$. At each location in this region ($r_0<r\leq a$) the ion distribution resembles two counterstreaming beams [see Eq. (19)]. The resonance at $u=1$ (corresponding to $v_s=v_{s'}$) in Fig. 3 describes collisions between particles that are comoving in the same beam. Collisions between comoving particles leads to strong coupling between the transverse and longitudinal velocity dispersion of these beams, as pointed out by Rosenberg and Krall.[11] We will return to this important effect in Sec. V. In this section we ignore the internal structure of these beams, focusing on the rate of increase in velocity dispersion due to collisions between ions in counterstreaming beams. We remove the effect of collisions between comoving ions from our representation of the collision integral by replacing the collision integral $I_\perp(\mu_0,u)$ with $I_\perp'(\mu_0,u)$, which has been cutoff at $\mu_c=0.95$, as described in the Appendix. In the bulk region [where $\mu_0=\sqrt{1-(r_0/r)^2}\approx 1$], this modified collision integral is well approximated by

$$\lim_{\mu_0\to 1}[I_\perp'(\mu_0,u)]=\frac{1}{2}\frac{1}{u_{s'}+1}. \tag{29}$$

The variation of $I_\perp(\mu_0,u)$ with particle speed in the plasma core ($r\leq r_0$) is shown in Fig. 4.

At a given radius the collisional rate of increase in L^2 is simply related to the collisional rate of increase in the transverse velocity dispersion,

$$\left.\frac{dL^2}{dt}\right|_{\text{collisions}}=m_s^2r^2\frac{d}{dt}\langle\Delta v_\perp^2\rangle. \tag{30}$$

The rate of increase in L^2 varies over the ion orbit. However, at the ion densities and energies projected for an IEC reactor the change in L^2 due to collisions during a single orbit is small. Hence, we average the collisional change in L^2 over the ion orbit to eliminate the rapid time scale associated with ion orbital motion, and obtain the bounce-averaged rate of change in L^2:

$$\left\langle\frac{d}{dt}L^2\right\rangle_{\text{collisions}}=\frac{1}{\tau_b}\int_0^a\frac{dr}{v_r}\left.\frac{dL^2}{dt}\right|_{\text{collisions}}. \tag{31}$$

The radial dependence of the transverse collision integral, $I_\perp'[\mu_0(r),u]$, is shown in Fig. 5. Except for a small region about the plasma core ($r\leq 3r_0$), $I_\perp'$ is well approximated by Eq. (29). Hence, the rate of increase in the transverse velocity dispersion depends on radius mainly through the ion density. We may isolate this dependence by multiplying and dividing by the ion density, and noting that the factor

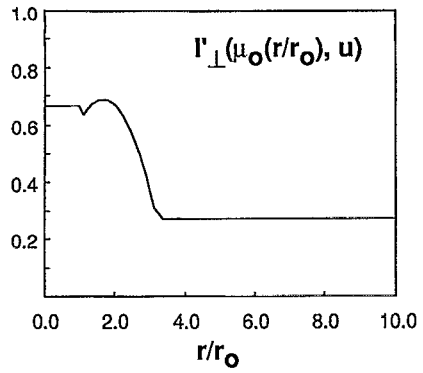

FIG. 5. Radial variation in the transverse collision integral, $I_\perp'[\mu_0(r),u]$ is displayed versus r/r_0 for a test particle with speed $u=1$. The structure at $r/r_0\approx 1$ is associated with the cutoff in $I_\perp'$ at $\mu_c=0.95$ applied for $r/r_0\geqslant 1$.

$(\nu_0^{s/s'}/n_{s'})$ is nearly independent of radius. Hence, we may approximate the bounce-average collisional rate increase in L^2 for ions of species s as

$$\frac{d}{dt}\langle L^2\rangle_{\text{collisions}}\approx m_s^2 v_s^2 \sum_{s'} \frac{\nu_0^{s/s'}}{n_{s'}} \frac{v_s}{|v_s+v_{s'}|} \times \int_0^a \frac{dr}{a} r^2 n_{s'}(r), \tag{32}$$

$$\approx c_s L_a^2 \langle n_s\rangle_{\text{Vol}} \left(\frac{\nu_0^{s/s}}{n_s}\right) \approx c_s L_a^2 \langle \nu_0^{s/s}\rangle_{\text{Vol}}, \tag{33}$$

where

$$c_s \equiv \sum_{s'} \frac{v_s}{|v_s+v_{s'}|}, \tag{34}$$

the sum on s' includes field ions of the opposite species streaming both parallel and anti-parallel to the test ions of species s; and $L_a^2=\frac{2}{3}(m_s v_s a)^2$ is the value of $\langle L^2\rangle$ for an isotropic, monoenergetic ion distribution—that is, an ion distribution that yields a constant ion density throughout the trap. For a DT plasma we find $c_d=6.5$ and $c_t\approx 5.4$.

We were motivated to introduced the volume-average scattering rate,

$$\langle \nu_0^{s/s'}\rangle_{\text{Vol}} \equiv \frac{4\pi q_s^2 q_{s'}^2 \,\text{Ln}\,\Lambda_{ss'}}{m_s^2 v_s^3} \langle n_{s'}\rangle_{\text{Vol}}, \tag{35}$$

because (assuming that the total number of ions is conserved) this rate is constant as the ion distribution function relaxes toward isotropy. It follows that the rate of increase in $\langle L^2\rangle$ is independent of time, and that, even after taking credit for the central concentration of the ion density, the ion distribution function relaxes to isotropy in a time[17]

$$\tau_L^s \approx \frac{1}{c_s \langle \nu_0^{s/s}\rangle_{\text{Vol}}}. \tag{36}$$

For the reference IEC reactor of Table I, this works out to $\tau_L^d\approx 69$ ms.

In the absence of particle sources and sinks, collisional effects define a minimum rate of at which the ion focus degrades. The actual rate of degradation can be substantially higher. For example, asymmetries in the confining potential may occur due to the inherent lack of symmetry in the magnetic fields needed to confine the electrons that generate the potential well,[18] asymmetries associated internal or external electrodes, asymmetries associated with the apparatus that injects the ions into the trap, or due to waves and instabilities.[19] Even very small asymmetries in the confining potential can substantially increase the rate at which the ion distribution function relaxes toward isotropy because they scatter longitudinal velocity into transverse velocity at a radius $r\approx a$ (so for a fixed $\Delta v_\perp^2$ we generate the maximum change in L^2); and because a "collision" occurs between each ion and the confining potential once each bounce period. Hence, we may estimate the rate of change in L^2 due to asymmetries in the confining potential as

$$\frac{d}{dt}\langle L^2\rangle_{\text{asymmetries}} \sim m\left(\frac{\delta\phi}{\phi_0}\right)\frac{1}{\tau_b}, \tag{37}$$

where "m" is the mode number and $\delta\phi$ is the magnitude of the asymmetry in the confining potential. For the 50 keV deuterons in the reference IEC reactor described in Table I, $1/\tau_b\approx 1.1$ MHz, while $\langle \nu_0^{d/d}\rangle_{\text{Vol}}\approx 2.23$ Hz. Hence, the bounce frequency is larger than the collision frequency by a factor of 7.6×10^4. Clearly, even very small asymmetries in the confining potential can lead to relaxation of the anisotropy in the ion distribution function at a faster rate than Coulomb collisions.

B. Collisional relaxation of the ion energy distribution

It is still important to examine the collisional relaxation of the monoenergetic ion energy distribution function because the rate of thermalization in energy has important implications regarding the effect of collisions between comoving ions on the evolution of the ion anisotropy (see Sec. V).

In the Appendix it is shown that the collisional rate of increase in the longitudinal velocity dispersion of ions of species "s" is given by

$$\frac{d}{dt}\langle \Delta v_\parallel^2\rangle_s = \sum_{s'} \nu_0^{s/s'} v_s^2 \frac{v_s}{v_{s'}} I_\parallel(\mu_0,u_{s'}). \tag{38}$$

The variation of the longitudinal collision integral with speed in the plasma core ($r\leqslant r_0$), is shown in Fig. 6. For $u\leqslant 1$, $I_\parallel(\mu_0=0,u)$ takes the same value ($\frac{2}{5}$) as the transverse collision integral, $I_\perp(\mu_0=0,u)$. Hence, the collisional diffusion is isotropic in the core at low ion velocity (as expected for an isotropic distribution function), while pitch angle scattering (and drag, which is not treated here) are the dominant collisional effects for fast particles.

Unlike the transverse collision integral, the longitudinal collision integral approaches zero in the bulk region ($r>r_0$), where it may be approximated by

$$I_\parallel'[\mu_0(r),u]\approx \frac{1}{4}\frac{(r_0/r)^2}{(1+u_{s'})^3} \quad (r\gg r_0). \tag{39}$$

Bussard[9] noted that bulk collisions would not cause energy diffusion if the energy of the heavier ion species is smaller than that of the lighter ion by exactly the ratio of the ion

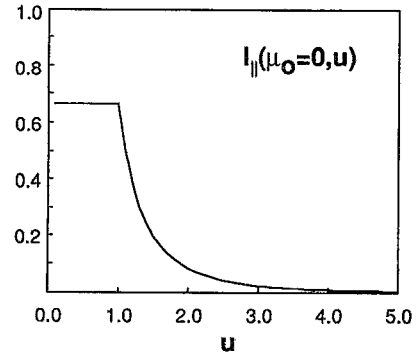

FIG. 6. Here $I_{\|}(\mu_0,u)$ is displayed as a function of test particle speed for $\mu_0=0$, corresponding to radial locations in the plasma core, $r\leqslant r_0$.

masses (when this condition is satisfied the center-of-mass frame is nearly identical to the lab frame for collisions between counterstreaming ions in the plasma bulk). The more general result of Eq. (39)—that collisions in the bulk plasma do not cause appreciable energy diffusion for any choice of the relative ion energies—follows from the assumption that the scattering angle is small (which is always the case for the dominant contribution to the Coulomb collision operator), together with the fact that, in the bulk plasma region, the velocities of the colliding particles are nearly colinear. For small-angle collisions the momentum transfer between the colliding particles can be obtained by treating the interaction as a perturbation, and integrating along the unperturbed (i.e., parallel, straight-line) orbits. When the impact parameter is finite (as required for small-angle collisions), it is easily seen that the momentum transfer (the time integral of the force on one particle due to interaction with the other particle) must be perpendicular to the particle velocities for any central force law. Hence, bulk collisions can produce pitch-angle scattering (as described by the transverse collision integral) but not energy diffusion, independent of the relative energies of the colliding ions. We conclude that only the plasma core contributes to the collisional increase in the longitudinal velocity dispersion. This is apparent in Fig. 7, which shows the radial dependence of $I_{\|}'(\mu_0,u)$.

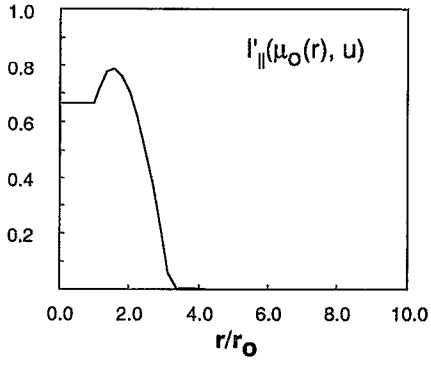

FIG. 7. Radial variation in the longitudinal collision integral, $I_{\|}'[\mu_0(r),u]$, is displayed for a test particle with speed $u=1$. The structure at $r/r_0\approx 1$ is associated with the cutoff in $I_{\|}'$ at $\mu_c=0.95$ applied for $r/r_0\geqslant 1$.

The bounce-averaged collisional rate of increase in the ion energy is

$$\langle \nu_\epsilon^s\rangle_{\text{orbit}}=\frac{v_s}{a}\int_0^a \frac{dr}{v_s}\frac{1}{v_s^2}\frac{d}{dt}\langle \Delta v_{\|}^2\rangle_s$$

$$\approx\sum_{s'}\frac{\nu_0^{s/s'}}{n_{s'}}\frac{v_s}{v_{s'}}\int_0^a\frac{dr}{a}n_{s'}(r)I_{\|}[\mu_0(r),u_{s'}] \tag{40}$$

$$\approx\frac{2}{3}d_s\left(\frac{a}{r_0}\right)\langle\nu_0^{s/s}\rangle_{\text{Vol}}, \tag{41}$$

where

$$d_s=\sum_{s'}\frac{v_s}{v_{s'}}\int_0^a\frac{dr}{r_0}\frac{n_{s'}(r)}{n_{s0}}I_{\|}\left(\mu_0(r),\frac{v_s}{v_{s'}}\right). \tag{42}$$

We have computed the orbit integral numerically for a DT plasma with equal deuterium and tritium fractions, finding $d_d\approx 1.73$ and $d_t\approx 1.91$.

At constant ion convergence ratio (a/r_0), the ion energy distribution would relax to a Maxwellian in a time of order,

$$\tau_\epsilon^s\approx\frac{3}{2d_s}\left(\frac{r_0}{a}\right)\frac{1}{\langle\nu_0^{s/s}\rangle_{\text{Vol}}}\ll\tau_L^s. \tag{43}$$

For our reference IEC reactor of Table I this works out to $\tau_\epsilon^d\approx 5.4$ ms.

V. COLLISIONS BETWEEN COMOVING IONS

When mapped to radial locations in the bulk plasma $(r_0<r<a)$ the model IEC ion distribution function of Sec. II yields a local ion distribution that corresponds to two ion beams counterstreaming at speeds $\pm v_s$ [see Eq. (19)]. In this section we consider the effect of collisions between ions in the same beam (that is, comoving ions) on the longitudinal and transverse velocity dispersion of that beam. In earlier work, Rosenberg and Krall[11] considered the collisional evolution of the ion distribution function in a model in which the confining potential has a finite gradient at the plasma surface. They point out that, for a nearly monoenergetic ion distribution function, the mean-squared ion velocity near the ion injection point (which is simply related to the longitudinal and transverse velocity dispersion discussed in Sec. IV) is small compared to ion streaming velocity, v_s. Hence, the ion collision frequency, which goes as $1/v^3$, will be large at the plasma surface. Rosenberg and Krall conclude that these edge collisions cause a relaxation of the longitudinal and transverse velocity dispersion toward isotropy $(\langle\Delta v_\perp^2\rangle_s\approx 2\langle\Delta v_{\|}^2\rangle_s)$ at a rate

$$\left.\frac{d\langle\Delta v^2\rangle}{dt}\right|_{\text{edge collisions}}\sim\frac{r_\phi}{a}\sqrt{\frac{q_s\phi_0}{m\langle\Delta v^2\rangle}}\,q_s\phi_0\langle\nu_0^{s/s}\rangle_{\text{Vol}}, \tag{44}$$

where

$$r_\phi\equiv\left(\frac{1}{\phi_0}\left.\frac{d\phi}{dr}\right|_{r=a}\right)^{-1} \tag{45}$$

is the potential gradient scale length at $r \approx a$. The effect of these edge collisions is to transfer energy between the longitudinal and transverse degrees of freedom. That is, to couple the energy spread of the ion beam to the quality of the ion focus.

Edge collisions are omitted from our square-well model because r_ϕ vanishes for a square well. However, collisions between comoving ions in the plasma bulk have the same effect—i.e., these collisions couple the longitudinal and transverse degrees of freedom, the collisional rate is large because the relative velocity of the comoving ions is small, and they act over most of the ion orbit, rather than just at the plasma surface. Collisions between comoving ions change the beam velocity dispersion at a rate

$$\left.\frac{d\langle \Delta v^2\rangle}{dt}\right|_{\text{comoving ions}} \sim \sqrt{\frac{q_s\phi_0}{m\langle \Delta v^2\rangle}}\, q_s\phi_0 \langle \nu_0^{s/s}\rangle_{\text{Vol}}. \tag{46}$$

Since r_ϕ/a is expected to be less than unity, we conclude that bulk collisions between comoving ions dominate the edge collisions emphasized in Ref. 11. These collisions are included in our square-well model, and will be examined in detail in the remainder of this section.

Following Rosenberg and Krall, we resolve the singularity associated with the delta function in the ion distribution function by modeling the internal structure of the beam-like ion distribution function in the plasma bulk by assuming that it is a drifting bi-Maxwellian. The longitudinal and transverse temperatures of the beam are chosen to reproduce the longitudinal and transverse velocity dispersion discussed in Sec. IV. The ion distribution function has a longitudinal velocity dispersion,

$$\langle \Delta v_\parallel^2\rangle \equiv \frac{T_\parallel^{(s)}}{m_s}, \tag{47}$$

and a transverse velocity dispersion,

$$\langle \Delta v_\perp^2\rangle(r) = \frac{\langle L^2\rangle}{m_s^2 r^2} \equiv \frac{2T_\perp^{(s)}(r)}{m_s}. \tag{48}$$

Note that the transverse velocity dispersion of the beam, $\langle \Delta v_\perp^2\rangle$, and the transverse temperature, $T_\perp^{(s)}$, are simply related to $\langle L^2\rangle$ and the ion focal radius, r_0 [see Eq. (49) below]. Hence, we only introduce one new parameter, $T_\parallel^{(s)}$, to describe the internal structure of the counterstreaming ion beams.

The transverse temperature, $T_\perp^{(s)}$, is a strong function of radius. This strong radial variation in $T_\perp^{(s)}$ results from the fact that different groups of ion orbits intersect at each radial location. Hence, we find it convenient to compute the contribution of collisions among comoving ions to the transverse velocity dispersion of the ion "beam" by relating it to $d\langle L^2\rangle/dt$. We may then compute the local value of $T_\perp^{(s)}(r)$ and the ion focal radius from the relations

$$T_\perp^{(s)}(r) = T_\perp^{(s)}(a)\,\frac{a^2}{r^2} = \frac{1}{2}\,q_s\phi_0\,\frac{r_0^2}{r^2} = \frac{\langle L^2\rangle}{2m_s r^2}. \tag{49}$$

In the absence of collisions between comoving ions, the velocity dispersion would increase at the (bounce-averaged) rates computed in Sec. IV. These rates of increase in the beam longitudinal temperature and $\langle L^2\rangle$ for ions of species s are

$$\left.\frac{dT_\parallel^{(s)}}{dt}\right|_{\text{core collisions}} \approx \frac{4}{3}\,d_s\left(\frac{a}{r_0}\right) q_s\phi_0\langle \nu_0^{s/s}\rangle_{\text{Vol}} \tag{50}$$

and

$$\left.\frac{d\langle L^2\rangle}{dt}\right|_{\text{bulk collisions}} \approx c_s L_a^2 \langle \nu_0^{s/s}\rangle_{\text{Vol}}. \tag{51}$$

A. Nearly monoenergetic ions, $(T_\parallel^{(s)}/q_s\phi_0) < \frac{1}{2}(r_0^2/a^2)$

We follow Kogan[20] in computing the collisional relaxation of the beam velocity dispersion between the longitudinal and transverse degrees of freedom. In the spirit of the model IEC ion distribution function of Sec. II, we begin by considering a beam with a finite ion convergence radius (so that $\langle L^2\rangle > 0$) and a nearly monoenergetic ion distribution function, such that $T_\perp^{(s)}(a) \geqslant T_\parallel^{(s)}$ or, equivalently, $T_\parallel^{(s)}/q_s\phi_0 < 0.5 r_0^2/a^2$. Then $T_\perp^{(s)} \geqslant T_\parallel^{(s)}$ everywhere in the well, and the local rates of change in $T_\perp^{(s)}$ and $T_\parallel^{(s)}$ due to collisions among comoving ions are[20]

$$\left.\frac{dT_\parallel^{(s)}}{dt}\right|_{\text{comoving ions}} \approx \sqrt{\pi}\left(\frac{r}{r_0}\right) q_s\phi_0\,\nu_0^{s/s} \tag{52}$$

and

$$\left.\frac{dT_\perp^{(s)}}{dt}\right|_{\text{comoving ions}} \approx -\frac{1}{2}\sqrt{\pi}\left(\frac{r}{r_0}\right) q_s\phi_0\,\nu_0^{s/s}. \tag{53}$$

It follows that the local rate of change in $\langle L^2\rangle$ due to collisions among comoving ions is

$$\left.\frac{d\langle L^2\rangle}{dt}\right|_{\text{comoving ions}} \approx -\frac{3}{4}\sqrt{\pi}\left(\frac{r^3}{a^2 r_0}\right) L_a^2\,\nu_0^{s/s}. \tag{54}$$

These rates need to be averaged over that portion of the ion trajectory with $r \gtrsim r_c$, where

$$r_c \equiv \frac{r_0}{\sqrt{1-\mu_c^2}} \approx 3.20\, r_0 \tag{55}$$

is the radius at which the cutoff in the longitudinal collisional integrals introduced in Sec. IV to remove the effect of collisions among comoving ions becomes effective (recall that we have taken $\mu_c \approx 0.95$). The orbit-averaged rates are

$$\left.\frac{dT_\parallel^{(s)}}{dt}\right|_{\text{comoving ions}} \approx \frac{\sqrt{\pi}}{4}\,\text{Ln}\left(\frac{a}{r_c}\right) \times \frac{4}{3}\left(\frac{a}{r_0}\right) q_s\phi_0\langle \nu_0^{s/s}\rangle_{\text{Vol}} \tag{56}$$

and

$$\left.\frac{d\langle L^2\rangle}{dt}\right|_{\text{comoving ions}} \approx -\frac{\sqrt{\pi}}{8}\left(\frac{a}{r_0}\right)\left(1-\frac{r_c^2}{a^2}\right) \times L_a^2\langle \nu_0^{s/s}\rangle_{\text{Vol}}. \tag{57}$$

Both core collisions and collisions among comoving ions lead to an increase in the longitudinal velocity dispersion. However, even for a relatively poorly focused ion distribution, $r_0/a < \sqrt{\pi}/8c_s \approx 0.21$, the decrease in $\langle L^2\rangle$ due to

collisions among comoving ions will dominate the increase due to collisions in the bulk plasma and $\langle L^2\rangle$ will decrease. As a result, the ion distribution will rapidly evolve until $T_\perp^{(s)}=T_\parallel^{(s)}$ at $r=a$.

B. Moderately thermalized ion distributions, $\frac{1}{2}(r_0^2/a^2)\leq T_\parallel^{(s)}/q_s\phi_0\leq\frac{1}{2}(r_0^2/r_c^2)$

We are led to consider the effects of collisions among comoving ions in the limit that the longitudinal velocity dispersion is large compared to the transverse velocity dispersion, $T_\parallel^{(s)}>T_\perp^{(s)}$. In this limit the local rates of change in $T_\parallel^{(s)}$ and $T_\perp^{(s)}$ due to collisions among comoving ions are[20]

$$\left.\frac{dT_\parallel^{(s)}}{dt}\right|_{\text{comoving ions}}\approx-\sqrt{\frac{2}{\pi}}\left(\frac{q_s\phi_0}{T_\parallel^{(s)}}\right)^{1/2}\times\text{Ln}\left(\frac{8T_\parallel^{(s)}}{q_s\phi_0}\frac{r^2}{r_0^2}\right)q_s\phi_0\nu_0^{s/s} \tag{58}$$

and

$$\left.\frac{dT_\perp^{(s)}}{dt}\right|_{\text{comoving ions}}\approx\sqrt{\frac{1}{2\pi}}\left(\frac{q_s\phi_0}{T_\parallel^{(s)}}\right)^{1/2}\times\text{Ln}\left(\frac{8T_\parallel^{(s)}}{q_s\phi_0}\frac{r^2}{r_0^2}\right)q_s\phi_0\nu_0^{s/s}. \tag{59}$$

It follows that the local rate of increase in $\langle L^2\rangle$ due to collisions among comoving ions is

$$\left.\frac{d\langle L^2\rangle}{dt}\right|_{\text{comoving ions}}\approx\sqrt{\frac{9}{8\pi}}\left(\frac{r^2}{a^2}\right)\left(\frac{q_s\phi_0}{T_\parallel^{(s)}}\right)^{1/2}\times\text{Ln}\left(\frac{8T_\parallel^{(s)}}{q_s\phi_0}\frac{r^2}{r_0^2}\right)L_a^2\nu_0^{s/s}. \tag{60}$$

We perform the orbit average by dividing the ion orbit into a portion at small radius, $r<r_x$, where $T_\perp^{(s)}(r)>T_\parallel^{(s)}$, and a portion at large r, $r>r_x$, where $T_\parallel^{(s)}>T_\perp^{(s)}(r)$, using the expressions for the local rate of change in the longitudinal and transverse temperatures appropriate for each region. The radius r_x, where $T_\perp^{(s)}(r_x)=T_\parallel^{(s)}$, is given by

$$r_x\equiv r_0\sqrt{\frac{q_s\phi_0}{2T_\parallel^{(s)}}}. \tag{61}$$

Averaging these rates over the ion orbit, we obtain expressions for the rates of change in the longitudinal and transverse beam temperatures valid for longitudinal beam temperatures in the range

$$\frac{1}{2}\frac{r_0^2}{a^2}\leq\frac{T_\parallel^{(s)}}{q_s\phi_0}\leq\frac{1}{2}\frac{r_0^2}{r_c^2}\approx5\times10^{-2},$$

$$\left.\frac{dT_\parallel^{(s)}}{dt}\right|_{\text{comoving ions}}\approx\frac{1}{\sqrt{\pi}}\left[\frac{\pi}{4}\text{Ln}\left(\frac{r_x}{r_c}\right)+\frac{r_x}{a}\text{Ln}\left(\frac{2e\,a}{r_x}\right)-\text{Ln}(2e)\right]\frac{4}{3}\left(\frac{a}{r_0}\right)q_s\phi_0\langle\nu_0^{s/s}\rangle_{\text{Vol}} \tag{62}$$

and

$$\left.\frac{d\langle L^2\rangle}{dt}\right|_{\text{comoving ions}}\approx\frac{1}{\sqrt{\pi}}\frac{r_xr_0}{a^2}\left[\text{Ln}\left(\frac{2a}{er_x}\right)-\frac{r_x}{a}\text{Ln}\left(\frac{2}{e}\right)-\frac{\pi}{8}\frac{a}{r_x}\left(\frac{r_x^2-r_c^2}{r_0^2}\right)\right]L_a^2\langle\nu_0^{s/s}\rangle_{\text{Vol}}, \tag{63}$$

where $e\approx2.718...$ is the base of the Naperian logarithms.

C. Strongly thermalized ion distributions, $T_\parallel^{(s)}/q_s\phi_0\geq\frac{1}{2}(r_0^2/r_c^2)$

Finally, we consider the regime $T_\parallel^{(s)}/q_s\phi_0\geq\frac{1}{2}(r_0^2/r_c^2)\approx5\times10^{-2}$. In this limit the longitudinal beam temperature is greater than the local value of the transverse beam temperature everywhere in the plasma bulk, and the orbit-averaged rates of change in the beam velocity dispersion are given by

$$\left.\frac{dT_\parallel^{(s)}}{dt}\right|_{\text{comoving ions}}\approx-\frac{1}{\sqrt{\pi}}\left[\frac{r_x}{r_c}\text{Ln}\left(\frac{2e\,r_c}{r_x}\right)-\frac{r_x}{a}\text{Ln}\left(\frac{2e\,a}{r_x}\right)\right]\frac{4}{3}\left(\frac{a}{r_0}\right)q_s\phi_0\langle\nu_0^{s/s}\rangle_{\text{Vol}} \tag{64}$$

and

$$\left.\frac{d\langle L^2\rangle}{dt}\right|_{\text{comoving ions}}\approx\frac{1}{\sqrt{\pi}}\frac{r_xr_0}{a^2}\left[\text{Ln}\left(\frac{2a}{e\,r_x}\right)-\frac{r_c}{a}\text{Ln}\left(\frac{2r_c}{e\,r_x}\right)\right]L_a^2\langle\nu_0^{s/s}\rangle_{\text{Vol}}. \tag{65}$$

D. Time evolution of $T_\parallel^{(s)}$, $\langle L^2\rangle$, and r_0/a

We are now ready to examine the time evolution of longitudinal velocity dispersion as measured by $T_\parallel^{(s)}/q_s\phi_0$, and the transverse velocity dispersion as measured by $\langle L^2\rangle$ or r_0/a. Summing the term describing the rate of increase in $T_\parallel^{(s)}$ due to core collisions [as given by Eq. (50)] with the appropriate term describing the rate of change in $T_\parallel^{(s)}$ due to both collisions between comoving ions [from Eq. (56), (62), or (64), as appropriate], we obtain an expression for the total rate of change in the longitudinal beam temperature,

$$\left.\frac{dT_\parallel^{(s)}}{dt}\right|_{\text{total}}=\frac{4}{3}G_s\left(\frac{T_\parallel^{(s)}}{q_s\phi_0},\frac{r_0}{a}\right)\left(\frac{a}{r_0}\right)q_s\phi_0\langle\nu_0^{s/s}\rangle_{\text{Vol}}. \tag{66}$$

The function $G_s(T_\parallel^{(s)}/q_s\phi_0,r_0/a)$ is displayed in Fig. 8 for deuterium ions in a DT plasma. We see that G_s is weakly varying with both $T_\parallel^{(s)}/q_s\phi_0$ and r_0/a. A further decrease in r_0/a beyond 10^{-4} results in only a very small downward shift relative to the $r_0/a=10^{-4}$ curve of Fig. 8; while at smaller values of $T_\parallel^{(s)}/q_s\phi_0$ the function G_s goes to

$$G_s\approx d_s+\frac{\sqrt{\pi}}{4}\text{Ln}\left(\frac{a}{r_0}\frac{r_0}{r_c}\right),\qquad\left(\frac{T_\parallel^{(s)}}{q_s\phi_0}<\frac{1}{2}\frac{r_0^2}{a^2}\right), \tag{67}$$

for any r_0/a. We find that $dT_\parallel^{(s)}/dt$ is positive for all values of $T_\parallel^{(s)}/q_s\phi_0$ and r_0/a. Hence, collisions will result in a monotonic increase of $T_\parallel^{(s)}$ with time.

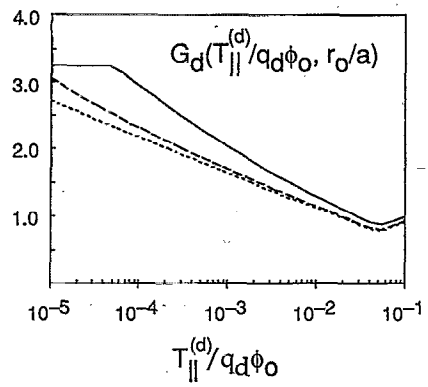

FIG. 8. The variation of the longitudinal beam heating rate, including both core collisions and collisions with comoving ions for deuterons in a DT plasma is displayed for $r_0/a=10^{-2}$ (solid line), $r_0/a=10^{-3}$ (long dashes), and $r_0/a=10^{-4}$ (short dashes).

The behavior of the transverse velocity dispersion as measured by $\langle L^2\rangle$ is more interesting. Summing the term describing the rate of increase in $\langle L^2\rangle$ due to core collisions [as given by Eq. (51)], with the appropriate term describing the rate of change in $\langle L^2\rangle$ due to both collisions between comoving ions [from Eqs. (57), (63), or (65), as appropriate] we obtain an expression for the total rate of change in the $\langle L^2\rangle$,

$$\left.\frac{d\langle L^2\rangle}{dt}\right|_{\text{total}} = H_s\left(\frac{T_{\|}^{(s)}}{q_s\phi_0}, \frac{r_0}{a}\right) L_a^2\langle \nu_0^{s/s}\rangle_{\text{Vol}}. \tag{68}$$

The function $H_s(T_{\|}^{(s)}/q_s\phi_0, r_0/a)$ is displayed in Fig. 9.

When $T_{\|}^{(s)}/q_s\phi_0$ is small (less than $0.017 r_0/a$ for deuterium in a DT plasma) collisions between comoving ions dominate the bulk plasma collisions so that the net effect is rapid decrease in $\langle L^2\rangle$ (i.e., a rapid decrease in the size of the ion focus, r_0). For the smallest values of $T_{\|}^{(s)}/q_s\phi_0 H_s$ asymptotes to

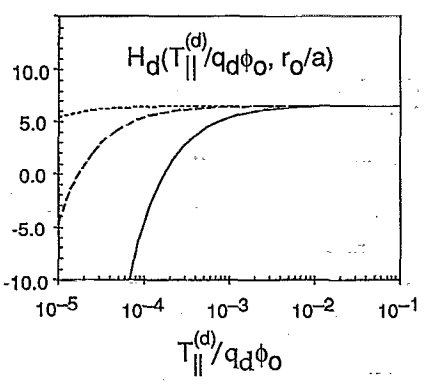

FIG. 9. The variation in the total transverse beam heating rate as measured by the rate of increase in $\langle L^2\rangle$, including both bulk collisions and collisions between comoving ions, is displayed for deuterium ions in a DT plasma with $r_0/a=10^{-2}$ (solid line), $r_0/a=10^{-3}$ (long dashes), and $r_0/a=10^{-4}$ (short dashes) as a function of $T_{\|}^{(d)}/q_d\phi_0$.

$$H_s \approx c_s - \frac{\sqrt{\pi}}{8}\frac{a}{r_0}, \quad \left(\frac{T_{\|}^{(s)}}{q_s\phi_0} < \frac{1}{2(r_0/a)^2}\right).$$

However, for larger values of $T_{\|}^{(s)}/q_s\phi_0$ the orbit-averaged effect of collisions between comoving ions weakens, so that both $\langle L^2\rangle$ and $T_{\|}^{(d)}$ increase monotonically with time when $T_{\|}^{(d)}/q_d\phi_0 > 0.017 r_0/a$.

The transition from collisional focusing to collisional defocusing can be understood by examining the leading terms in the expression for $d\langle L^2\rangle/dt$ in the moderately thermalized regime, $\frac{1}{2}r_0^2/a^2 \leq T_{\|}^{(s)}/q_s\phi \leq \frac{1}{2}(r_0^2/r_c^2)$,

$$\left.\frac{d\langle L^2\rangle}{dt}\right|_{\text{total}} \approx \left[c_s - \frac{\sqrt{\pi}}{16}\frac{q_s\phi_0}{T_{\|}^{(s)}}\left(\frac{r_0}{a}\right)\right] L_a^2\langle \nu_0^{s/s}\rangle_{\text{Vol}}, \tag{69}$$

where we have used Eq. (61) to express $(r_\chi/r_0)^2$ as $\frac{1}{2}T_{\|}^{(s)}/q_s\phi_0$. It follows that the transition from focusing to defocusing for deuterium in a DT plasma occurs when

$$\frac{T_{\|}^{(d)}}{q_s\phi_0} \approx \frac{\sqrt{\pi}}{16 c_d}\frac{r_0}{a} \approx 0.017\,\frac{r_0}{a}. \tag{70}$$

After initial transients, in which the ion focal radius may decrease in size while $T_{\|}^{(s)}/q_s\phi_0$ increases, the system will reach a state in which $T_{\|}^{(s)}/q_s\phi_0 \gtrsim r_0/a$. The longitudinal temperature and ion convergence then satisfy the equations

$$\frac{d}{dt}\left(\frac{T_{\|}^{(s)}}{q_s\phi_0}\right) \approx 1.7\left(\frac{r_0}{a}\right)^{-1}\langle \nu_0^{s/s}\rangle_{\text{Vol}}, \tag{71}$$

where we have taken $G_d \approx 1.3$ (valid for and $T_{\|}^{(s)}/q_s\phi_0 \sim r_0/a \gtrsim 10^{-2}$; see Fig. 8); and

$$\frac{d}{dt}\left(\frac{r_0}{a}\right) \approx 4.3\left(\frac{r_0}{a}\right)^{-1}\langle \nu_0^{s/s}\rangle_{\text{Vol}}, \tag{72}$$

where we have taken $H_d \approx 6.4$ (valid for $T_{\|}^{(d)}/q_d\phi_0 \gtrsim r_0/a$; see Fig. 9), and eliminated $\langle L^2\rangle$ in favor of r_0/a using Eqs. (49).

These equations have the solution

$$\frac{r_0}{a} \approx 2.9\sqrt{\langle \nu_0^{d/d}\rangle_{\text{Vol}} t} \tag{73}$$

and

$$\frac{T_{\|}^{(d)}}{q_d\phi_0} \approx 1.2\sqrt{\langle \nu_0^{d/d}\rangle_{\text{Vol}} t} + \frac{T_{\|0}^{(d)}}{q_d\phi_0}. \tag{74}$$

We conclude that collisions between counterstreaming ions will initially lead to rapid thermalization of the distribution of ion radial velocities [at a rate of order $(a/r_0)\langle \nu_0^{s/s}\rangle_{\text{Vol}}$]. Once $T_{\|}^{(s)}$ has increased to the extent that $T_{\|}^{(s)}/q_s\phi_0 \gtrsim 0.017 r_0/a$ this process will be accompanied by the spreading of the ion focus. Finally, when $T_{\|}^{(s)}/q_s\phi_0 \gtrsim r_0/a$, the increase in $T_{\|}^{(s)}/q_s\phi_0$ and r_0/a will proceed in concert at a rate of order $(a/r_0)\langle \nu_0^{s/s}\rangle_{\text{Vol}}$. As the ion focus spreads the rate of increase in the focal radius decreases so that it takes a time of order

$$\tau_L^s \sim 0.12\langle \nu_0^{s/s}\rangle_{\text{Vol}}^{-1},$$

for the ion distribution function to relax to isotropy and for the IEC configuration to be destroyed.

Our conclusions regarding the time evolution of the IEC distribution function is very different from that reached in Ref. 11, where steady-state, beam-like solutions to the kinetic equation were found. Two key reasons for our completely different results are the following.

(1) The artificial constraint imposed in Eq. (11) of Ref. 11, which prevents collisions between counterstreaming ion beams from producing any net increase in the velocity dispersion (i.e., heating) of the ion beams

(2) The neglect of the dominant term in the evolution of the beam temperature—the increase in the longitudinal velocity dispersion of the beam due to collisions in the plasma core.

When this problem is treated correctly we see that there are no beam-like steady-state solutions to the kinetic equation.

VI. SCHEMES FOR MAINTAINING A STRONGLY FOCUSED ION DISTRIBUTION THAT DO NOT WORK

We have shown that ion–ion collisions will cause the IEC distribution to relax toward an isotropic Maxwellian. At the high energies and relatively low volume-averaged densities proposed for IEC devices, the ion collisional time scale is rather long—$\langle \nu_0^{d/d} \rangle_{\mathrm{Vol}}$ is about 2.2 Hz (as compared to an ion bounce frequency of 1.1 MHz)—for the IEC reactor parameters of Table I. Hence, it may be possible to prevent this collisional relaxation through some process that acts only weakly on the ion distribution function. We consider two such schemes that have been proposed by proponents of IEC fusion reactors in this section.

A. Fusion reaction rates

Bussard[9] makes the rather surprising claim that the fusion reactions in an IEC device will remove fuel ions at a rate sufficient to maintain a nearly monoenergetic ion distribution function. In making this claim Bussard recognizes that the fusion reaction rate must be greater than the collisional energy-scattering rate if the loss of fuel ions by fusion reactions is to substantially alter the ion distribution function. In Sec. V we showed that the orbit-averaged collisional rate of increase in the beam velocity dispersion is

$$\langle \nu_\epsilon^d \rangle_{\mathrm{orbit}} = \frac{1}{2} \frac{d}{dt} \frac{T_\parallel^{(s)}}{q_s \phi_0}\bigg|_{\mathrm{total}} \approx \frac{2}{3} d_d \left\langle \frac{a}{r_0} \right\rangle \langle \nu_0^{d/d} \rangle_{\mathrm{Vol}}, \tag{75}$$

while the orbit-averaged fusion rate for the deuterons is given by

$$\langle n_t \langle \sigma v \rangle_{\mathrm{DT}} \rangle_{\mathrm{orbit}} \approx \frac{v_0}{a} \int_0^a \frac{dr}{v_0} n_t(r) \langle \sigma v \rangle_{\mathrm{DT}}. \tag{76}$$

Note that the orbit-averaged fusion rate scales with the core convergence ratio and ion density as $(a/r_0)\langle n_i \rangle_{\mathrm{Vol}}$—that is, in exactly the same manner as the rate of increase in the longitudinal velocity dispersion. We computed the orbit-averaged fusion rate following the methods described in Sec. III. This rate is plotted, together with the orbit-averaged energy diffusion rate versus the potential well depth in Fig. 10. We see that the orbit-averaged energy diffusion rate substantially exceeds the orbit-averaged fusion rate at all potential well depths considered (5 kV$\leqslant \phi_0 \leqslant$300 kV). We conclude that fusion reactions rates are not sufficient to materially effect the form of the ion energy distribution function.

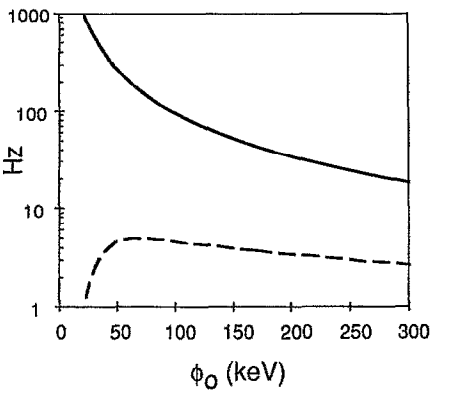

FIG. 10. An orbit-averaged fusion rate coefficient (solid curve) and orbit-averaged energy diffusion rate (dashed curve) versus potential well depth, ϕ_0, for deuterons in a DT plasma. The ion density, convergence ratio, etc. are taken from Table I. However, the relative magnitude of fusion and collisional rates are insensitive to these parameters.

The time required for complete relaxation of the ion anisotropy is longer (by $\sim a/r_0$) than the instantaneous time scale for spreading of the ion energy distribution. Hence, one might hope that the loss of fuel ions through fusion reactions could maintain the ion anisotropy. We may estimate the resulting ion core radius by replacing "t" in Eq. (73) with the inverse of the orbit-averaged fusion reaction rate. After a bit of manipulation, this estimate takes the form

$$\frac{r_0}{a} \approx 7.3 \frac{\langle \nu_\parallel^d \rangle_{\mathrm{orbit}}}{\langle n_t \langle \sigma v \rangle_{\mathrm{DT}} \rangle_{\mathrm{orbit}}} \gg 1. \tag{77}$$

We conclude that the removal of fuel ions by fusion reactions occurs at a rate that is insufficient to maintain an ion focus. The situation regarding maintenance of the ion anisotropy is essentially the same as that regarding maintenance of a non-Maxwellian ion energy distribution because the orbit-averaged fusion rate decreases as the ion focus spreads, thereby making fusion reactions less effective as a mechanism for removing fuel ions before they are scattered further in angle.

B. Maintenance of ion anisotropy with a "cold" plasma mantle

The basic idea inspiring the work of Rosenberg and Krall was that it might be possible to control the ion distribution function in an IEC device by manipulating the ion distribution function in the neighborhood of the ion injection point. In Sec. V we demonstrated that the calculation performed in Ref. 11 is in error, and that collisions between ions with low relative velocities cannot prevent thermalization of the ion distribution function. However, perhaps this only demonstrates that the wrong problem was addressed both in Sec. V and in Ref. 11. In this section we consider the related problem in which the ion distribution function at the injection point is treated as a boundary condition. We are then able to force the transverse temperature to go to zero at the

lip of the potential well, which we now take at $(\epsilon - L^2/2m_s a^2) = 0$ [rather than at $(\epsilon - L^2/2m_s a^2) = +q_s\phi_0$], so that this boundary condition will have greater influence on the distribution of trapped ions.

It is convenient to adopt as velocity-space coordinates u, the particle speed normalized to the thermal velocity, and μ, the cosine of the angle that the particle makes with the normal when it strikes the surface of the spherical square-well potential. Note that both of these velocity-space coordinates can be expressed as functions of ϵ and L^2,

$$\mu = \pm \sqrt{1 - \frac{L^2}{2m_s a^2(\epsilon + q_s\phi_0)}}, \tag{78}$$

$$u = \sqrt{\frac{2(\epsilon + q_s\phi_0)}{T_s}}, \tag{79}$$

so that u and μ are themselves constants of the single-particle motion. We assume that the steady-state ion distribution function is nearly an isotropic Maxwellian (and verify this assumption *a posteriori*), so that we may use the usual test-particle collision operator. In the high-velocity limit ($u \gtrsim 2$) the steady-state kinetic equation may then be written as

$$\frac{\partial^2 f}{\partial u^2} + \left(u - \frac{1}{u}\right)\frac{\partial f}{\partial u} + \frac{\partial}{\partial \mu}(1-\mu^2)\frac{\partial f}{\partial \mu} = 0. \tag{80}$$

We look for solutions in the form

$$f(u,\mu) = \sum_L f_L(u) P_L(\mu), \tag{81}$$

where the $P_L(\mu)$ are Legendre polynomials of index L, and the $f_L(u)$ satisfy

$$\frac{d^2 f_L}{du^2} + \left(u - \frac{1}{u}\right)\frac{df_L}{du} + L(L+1) f_L = 0. \tag{82}$$

We solve this equation on the domain $0 \leq u \leq u_{\max} = \sqrt{2q_s\phi_0/T_s}$, taking as our boundary condition a plasma with finite phase-space density and zero velocity spread at the ion injection point,

$$f(u_{\max},\mu) = \frac{f_0}{2}[\delta(\mu - 1) + \delta(\mu + 1)]. \tag{83}$$

Expanding this boundary condition in a Legendre series, we obtain $f_L(u_{\max}) = f_0(L + \frac{1}{2})$ for L even, and $f_L(u) = 0$ for L odd.

The solutions of the kinetic equation with this boundary condition are shown in Fig. 11 for the first four even Legendre harmonics. We see that our highly anisotropic boundary condition has an appreciable effect on the distribution function only at the highest speeds, $u \gtrsim 2$. The $L = 0$ Legendre harmonic, $f_0(u)$, is the sum of a Maxwellian plus a small constant term required to match the boundary condition at $u = u_{\max}$. The density and temperature of this Maxwellian must be determined from consideration of energy and particle balance in analogy to the Pastukhov solution of the problem of electron confinement in magnetic mirrors.[21,22]

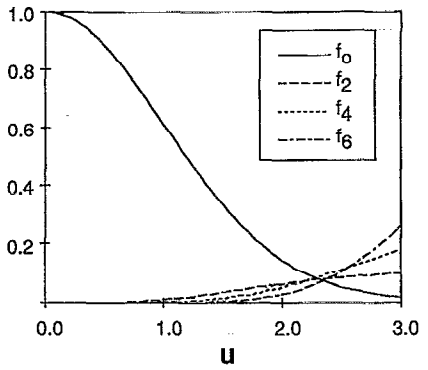

FIG. 11. The first four even Legendre harmonics of the steady-state ion distribution function when a zero transverse temperature boundary condition is applied at $u = 3$.

The bulk of the phase-space density is contained in $f_0(u)$, providing the *a posteriori* justification for the use of the test particle collision operator.

The effective radius of the ion focus may be computed as a function of the ion speed from the root-mean-square value of the distance of closest approach,

$$r_{\text{eff}}(u) \equiv a\sqrt{\frac{3}{2}\langle(1-\mu^2)\rangle(u)} = a\sqrt{\frac{f_0(u) - \frac{1}{5}f_2(u)}{f_0(u)}}. \tag{84}$$

We see that there is essentially no ion focusing at speeds less than twice the ion thermal velocity. We conclude that it is not possible to maintain a strongly anisotropic ion distribution function in an IEC device solely by controlling the form of the ion distribution function at the ion injection point.

VII. SCHEMES FOR MAINTAINING A STRONGLY FOCUSED ION DISTRIBUTION THAT WORK, BUT REQUIRE TOO MUCH POWER

We have shown that two mechanisms proposed by proponents of IEC systems to maintain a strongly nonthermal ion distribution function will not be effective. In the absence of intervention the ion distribution function will thermalize in an ion–ion collision time. In this section we propose an approach for maintaining a strong ion focus in an IEC system based on the assumption that some means can be found to control the ion lifetime in the electrostatic trap, i.e., we assume that ions can be intentionally "pumped" out of the electrostatic trap before they have time to fully thermalize. Such schemes are plausible since the ion lifetime is in fact limited in electrostatic traps that use grids (due to the finite grid transparency), and in Penning traps (due the leakage of ions through the poles of the trap). Similar schemes were proposed (and studied extensively), in connection with maintaining an anisotropic ion distribution in the thermal barrier cell of tandem mirrors.[23]

A. Power required to "pump" the ion distribution

When an ion is pumped from the trap it is replaced by an ion with zero angular momentum and zero energy (i.e., with an ion whose kinetic energy within the potential well is $q_s\phi_0$). Assuming that the lifetime of a typical ion is τ_{pump},

we can model the effects of ion pumping by adding appropriate sink terms to Eqs. (66) and (68), yielding

$$\left.\frac{dT_{\parallel}^{(s)}}{dt}\right|_{\text{total}} = \frac{4}{3} G_s\left(\frac{a}{r_0}\right) q_s \phi_0 \langle \nu_0^{s/s}\rangle_{\text{Vol}} - \frac{T_{\parallel}^{(s)}}{\tau_{\text{pump}}} \tag{85}$$

and

$$\left.\frac{d\langle L^2\rangle}{dt}\right|_{\text{total}} = H_s L_a^2 \langle \nu_0^{s/s}\rangle_{\text{Vol}} - \frac{\langle L^2\rangle}{\tau_{\text{pump}}}. \tag{86}$$

Equations (85) and (86) have the steady-state solution

$$\frac{r_0}{a} = \sqrt{\frac{4}{3} H_s \langle \nu_0^{s/s}\rangle_{\text{Vol}} \tau_{\text{pump}}} \tag{87}$$

and

$$\frac{T_{\parallel}^{(s)}}{q_s \phi_0} = \frac{G_s}{H_s}\frac{r_0}{a}, \tag{88}$$

where Eq. (49) was used to eliminate $\langle L^2\rangle$ in favor of r_0/a.

In these steady-state solutions the two parameters describing the ion distribution function (r_0/a and $T_{\parallel}^{(s)}/q_s\phi_0$) are replaced by a single parameter, [τ_{pump} in Eqs. (87) and (88)]. Alternatively, we may choose r_0/a as the single parameter characterizing the steady-state ion distribution function. Equation (87) then determines the required pumping time,

$$\tau_{\text{pump}} = \frac{3}{4}\frac{1}{H_s}\frac{(r_0/a)^2}{\langle \nu_0^{s/s}\rangle_{\text{Vol}}}, \tag{89}$$

while Eq. (88) determines the longitudinal velocity dispersion at the chosen convergence ratio. Equation (88) has been solved numerically (including the weak dependence of G_s and H_s on r_0/a and $T_{\parallel}^{(s)}/q_s\phi_0$ illustrated in Figs. 8 and 9) to determine $G_s(r_0/a)$ and $H_s(r_0/a)$ for these steady-state solutions. The residual dependence on the convergence ratio is weak—for deuterons in a DT plasma, G_d increases monotonically from 1.56 to 2.40 and H_d decreases monotonically from 6.3 to 6.21 as r_0/a decreases from 10^{-1} to 10^{-4}. For the IEC reactor parameters of Table I ($r_0/a = 10^{-2}$), we obtain $G_d \approx 1.69$, $H_d \approx 6.12$, $T_{\parallel}^{(d)}/q_d\phi_0 \approx 2.8\times 10^{-3}$, and $\tau_{\text{pump}} \approx 5.5\ \mu$s.

The energy required to remove an ion from the trap is estimated by the energy spread in the ion distribution,

$$\epsilon_{\text{pump}} \gtrsim m_s v_s \langle \Delta v_{\parallel}^2\rangle^{1/2} = q_s\phi_0 \sqrt{2\frac{T_{\parallel}^{(s)}}{q_s\phi_0}}. \tag{90}$$

Lower values of ϵ_{pump} are thermodynamically allowed,[24] but is very difficult to see how lower pumping energies could be achieved in IEC systems as they have been described in the literature to date. Assuming a potential well depth of $\phi_0 \approx 50.7$ keV to maximize the DT fusion rate coefficient, it will require about 3.8 keV to remove each ion.

The total power required to maintain the ion distribution function is then

$$P_{\text{pump}} \gtrsim \frac{N_i \epsilon_{\text{pump}}}{\tau_{\text{pump}}} \approx \left(\frac{32}{9} G_d H_d\right)^{1/2} q\phi_0 N_i \left(\frac{a}{r_0}\right)^{3/2} \langle \nu_0^{d/d}\rangle_{\text{Vol}}, \tag{91}$$

which comes to about 23 GW for the IEC reactor of Table I (which produces only 590 MW of fusion power).

The power balance in this operating mode can be characterized by the fusion gain,

$$Q_{\text{DT}} \lesssim \frac{P_{\text{fusion}}}{P_{\text{pump}}} \approx \frac{1}{\sqrt{18 G_d H_d}} \frac{Y_{\text{DT}}}{q_d\phi_0} \sqrt{\frac{r_0}{a}} \frac{\langle n_d\rangle_{\text{Vol}} \langle \sigma v\rangle_{\text{DT}}^{\text{eff}}}{\langle \nu_0^{d/d}\rangle_{\text{Vol}}}. \tag{92}$$

For the IEC reactor of Table I, we find $Q_{\text{DT}} \lesssim 0.026$. In fact, Q_{DT} will certainly be below this limit, as this estimate does not take account of the power required to maintain the potential well and support energy losses in the electron channel.

The estimate of the upper limit on the fusion gain depends on the potential well depth, ϕ_0, only through the combination

$$\langle \sigma v\rangle_{\text{DT}}^{\text{eff}} / (q_d \phi_0 \langle \nu_0^{d/d}\rangle_{\text{Vol}}) \sim \phi_0^{1/2} \langle \sigma v\rangle_{\text{DT}}^{\text{eff}}.$$

Numerical evaluation shows this to be a very slowly increasing function of ϕ_0 for $\phi_0 \gtrsim 50$ kV. The value increases by 10% as ϕ_0 is increased from 50 kV to 75 kV; and by an additional 10% as ϕ_0 is increased to 300 kV. Assuming that there must be some penalty to increasing ϕ_0, we take $\phi_0 \approx 75$ kV, yielding a 10% improvement in Q_{DT} (to $Q_{\text{DT}} \lesssim 0.028$). The fusion gain also increases with *decreasing* ion convergence ratio, a/r_0. Since a high ion convergence ratio is a defining feature of IEC systems, we will require $a/r_0 \gtrsim 10$. The fusion gain is then limited to $Q_{\text{DT}} \lesssim 0.091$.[25]

B. Effect of a "hard core" on pumping power requirements

It has been suggested[26] that the ion pumping power requirements can be mitigated by introducing a "hard core" in the electrostatic potential profile. We note that it is not entirely clear how such a hard core is to be established since the ion charge producing this hard core must be provided by ions that have sufficient energy to traverse the core (so these ions, at least, will undergo energy diffusion due to core collisions). Nevertheless, we devote this section to estimating the ion pumping requirements that would pertain if such a hard core potential can be produced.

It was concluded in Sec. IV B that a leading cause of ion energy diffusion in IEC devices is collisions in the vicinity of the plasma core. This effect can be removed by setting the coefficient d_s equal to zero. Note that this does not entirely eliminate ion energy diffusion—there remains the contribution to ion energy diffusion from bulk collisions between comoving ions, as described in Sec. V. The analysis of the pumping power requirements presented in the previous section still applies. However, the residual dependence of G_d and H_d must be recomputed with d_d set equal to zero. We find that G_d now varies from 0.361 to 0.889 and H_d varies

from 5.15 to 5.78 as r_0/a decreases from 10^{-1} to 10^{-4}. The optimized fusion gain (which still occurs at $r_0/a=0.1$ and $\phi_0 \approx 75$ kV) is increased to $Q_{DT} \leq 0.21$.

These very disappointing limits on the fusion gain follow from the fact that the averaged fusion rate is small compared to the averaged collisional rate [see Eq. (92) and Fig. 10], so that the power required to maintain the nonthermal IEC ion distribution is substantially larger than the fusion power generated. The IEC reactor power balance is optimized by allowing the ion distribution to thermalize as much as is consistent with the operating regime in question (i.e., choosing the lowest ion convergence ratio, a/r_0, consistent with an IEC configuration). The power required to maintain an ion distribution function that retains the defining characteristic of an IEC system ($a/r_0 \gtrsim 10$) is 11 times greater than the fusion power that this system might produce. If a "hard core" potential can be formed the reactor performance can be improved by a further factor of 2.3 to $Q_{DT} \lesssim 0.21$. Reactor studies indicate that an economic DT fusion power reactor requires a much more favorable energy balance, $Q_{DT} \gtrsim 10$. Hence, there appears to be no prospect that an economic electrical power generating reactor can be developed based on an inertial electrostatic confinement scheme.

VIII. CONCLUSIONS

We have presented a model for the ion distribution function in an inertial electrostatic confinement system. This model is shown to reproduce the essential features of IEC systems—electrostatic confinement, strong central peaking of the ions, and a nearly monoenergetic energy distribution. Using this model distribution function we are able to test key claims made by proponents of IEC systems. We find the following:

(1) After averaging over collision angle and volume, the peak in the effective fusion rate coefficient for DT ($\langle \sigma v \rangle_{DT}^{eff} \approx 9.0 \times 10^{-22}$ m^3/s at $\phi_0 \approx 50$ keV for the IEC distribution versus 8.9×10^{-22} m^3/s at $T=75$ keV for a thermal distribution) or D^{3}He ($\langle \sigma v \rangle_{D^3He}^{eff} \approx 2.8 \times 10^{-22}$ m^3/s at $\phi_0 \approx 140$ keV vs 2.5×10^{-22} m^3/s at $T=250$ keV) reactions are not significantly higher than the peak in the corresponding thermal rate coefficient.

(2) Ion/ion collisions will cause the ion distribution function to relax toward a Maxwellian at an instantaneous rate that is enhanced relative to the ion–ion collision frequency (evaluated at the volume-averaged density) by one power of the convergence ratio, a/r_0.

(3) In the absence of a competing process, the ion distribution will fully relax to an isotropic Maxwellian on the ion–ion collisional time scale (evaluated at the volume-averaged density).

(4) The means of preventing this relaxation of the ion distribution function so far proposed by proponents of IEC schemes are not effective.

(5) The energy cost of maintaining an anisotropic ion distribution function through control of the ion lifetime is greater than the fusion power that would be produced by the IEC device.

This analysis is based on a particular model ion distribution function. While the reactor operating point has been optimized over the parameters of this model, it is possible that a more attractive power balance could be obtained by further optimization of the form of the ion distribution function. A serious effort to perform such an optimization would require the development of a bounce-averaged Fokker Planck code in (ϵ, L^2) space. However, it seems most unlikely that such optimization will increase Q by the factor of ~ 100 (or ~ 50 if hard core potentials can be maintained) required to achieve an acceptable recirculating power fraction for an economic power plant. Hence, we conclude that inertial electrostatic confinement shows little promise as a basis for the development of commercial electrical power plants.

The analysis does not place a lower limit on the unit size of an IEC reactor. Such a lower limit on the unit size will (presumably) follow from an analysis of electron energy confinement and the energy cost of maintaining the spherical potential well. This leaves open the possibility that IEC-based reactors may prove useful as a means of generating a modest flux of 14 MeV neutrons for applications other than power generation, such as such as assaying, neutron imaging, materials studies, and isotope production. In such applications a small unit size ($P_{fusion} \lesssim 1$ kW) and, hence, smaller unit cost might compensate for modest values of Q_{DT}.

ACKNOWLEDGMENTS

This work was motivated by presentations of R. W. Bussard and N. A. Krall on the promise of IEC-based fusion reactors. It has benefited from stimulating discussions with B. Afeyan, D. C. Barnes, R. H. Cohen, T. J. Dolan, R. Durst, R. Fonck, T. K. Fowler, L. L. Lodestro, G. H. Miley, J. Perkins, T. Rider, and D. Ryutov. Particular thanks are due to S. W. Haney for providing the numerical solution to the ion kinetic equation described in Sec. VI.

This work was performed under the auspices of the U.S. Department of Energy by the Lawrence Livermore National Laboratory under Contract No. W-7405-ENG-48.

APPENDIX: COLLISIONAL RATE COEFFICIENTS FOR A MONOENERGETIC IEC DISTRIBUTION FUNCTION

In this appendix we compute the rate of increase in the transverse and longitudinal velocity dispersion, $\langle \Delta v_\perp^2 \rangle$ and $\langle \Delta v_\parallel^2 \rangle$, for a test particle of species s and velocity $\mathbf{v}=v_r \hat{\mathbf{e}}_r$, colliding with field particles of species s'. The distribution function of the field particles is taken to be the monoenergetic IEC model distribution function defined in Sec. II. Since the model IEC velocity distribution function varies as a function of radius, we expect these rates of increase in the longitudinal and transverse velocity dispersion to vary with radius.

Rosenbluth, McDonald, and Judd[27] give a compact expression for the rate of increase in the velocity dispersion due to Coulomb collisions. Following these authors we use the symbols $\langle \Delta v_\perp^2 \rangle$ and $\langle \Delta v_\parallel^2 \rangle$ in this appendix only to denote the rate of increase in the velocity dispersion rather than the

velocity dispersion itself. In the main text these symbols are used to denote the velocity dispersion. These rates are given by

$$\langle \Delta \mathbf{v}\, \Delta \mathbf{v}\rangle_s = \sum_{s'} \langle \Delta \mathbf{v}\, \Delta \mathbf{v}\rangle_{ss'},$$

where $\langle \Delta \mathbf{v}\, \Delta \mathbf{v}\rangle_{ss'}$, the rate of increase in the velocity dispersion in species s due to collisions with particles of species s', is given by

$$\langle \Delta \mathbf{v}\, \Delta \mathbf{v}\rangle_{ss'} = \frac{4\pi q_s^2 q_s^2 \,\mathrm{Ln}\,\Lambda_{ss'}}{m_s^2} \frac{\partial^2}{\partial \mathbf{v}\,\mathbf{v}} \int d^3\mathbf{v}'\, f_{s'}(\mathbf{v}') \times |\mathbf{v}-\mathbf{v}'|.$$

Defining characteristic speeds v_s for species s, and using the vector identity

$$\frac{\partial^2}{\partial \mathbf{v}\,\mathbf{v}} |\mathbf{v}-\mathbf{v}'| = \frac{\mathbf{I}-\hat{\mathbf{w}}\hat{\mathbf{w}}}{|\mathbf{w}|},$$

we can write the rate of increase in the velocity dispersion as

$$\langle \Delta \mathbf{v}\, \Delta \mathbf{v}\rangle_{ss'} = \nu_0^{s/s'} v_s^2 \frac{v_s}{n_{s'}} \int d^3\mathbf{v}'\, f_{s'}(\mathbf{v}') \frac{\mathbf{I}-\hat{\mathbf{w}}\hat{\mathbf{w}}}{|\mathbf{w}|},$$

where $\mathbf{w} \equiv (\mathbf{v}-\mathbf{v}')$, $\hat{\mathbf{w}} \equiv \mathbf{w}/|\mathbf{w}|$, $\mathbf{I}$ is the identity tensor, and, following Book,[16] we define

$$\nu_0^{s/s'} \equiv \frac{4\pi q_s^2 q_{s'}^2 n_{s'} \,\mathrm{Ln}\,\Lambda_{ss'}}{m_s^2 v_s^3}.$$

The monoenergetic IEC distribution evaluated at radius r may be written in spherical coordinates as

$$f_{s'}(\mathbf{v}') = \frac{n_{s'}(r)}{2\pi v_{s'}^2} \frac{H(|\mu'|-\mu_0)}{2(1-\mu_0)} \delta(v'-v_{s'}),$$

where the principle axis of the spherical coordinates is taken parallel to $\hat{\mathbf{e}}_\mathbf{r}$, μ' is the cosine of the angle between $\mathbf{v}'$ and $\hat{\mathbf{e}}_\mathbf{r}$, $n_{s'}(r)$ is the local value of the field ion density as given by Eq. (9),

$$v_{s'} = \sqrt{\frac{2q_{s'}\phi_0}{m_{s'}}}$$

and

$$\mu_0 = \begin{cases} 0, & r \leq r_0, \\ \sqrt{1-r_0^2/r^2}, & r > r_0. \end{cases}$$

The integral over the field ion speed is easily performed, yielding

$$\langle \Delta \mathbf{v}\, \Delta \mathbf{v}\rangle_{ss'} = \nu_0^{s/s'} v_s^2 \frac{v_s}{v_{s'}} \int_{-1}^{1} d\mu' \int_0^{2\pi} \frac{d\phi}{2\pi} \frac{H(|\mu'|-\mu_0)}{2(1-\mu_0)} \times \frac{\mathbf{I}-\hat{\mathbf{w}}\hat{\mathbf{w}}}{\sqrt{1+u_{s'}^2-2\mu' u_{s'}}},$$

where

$$u_{s'} \equiv v_s / v_{s'}.$$

The only dependence on the azimuthal angle, ϕ, comes through the unit vector

$$\hat{\mathbf{w}} = \frac{(u_{s'}-\mu')\hat{\mathbf{e}}_\mathbf{r} - \sqrt{1-\mu'^2}(\hat{\mathbf{e}}_1 \cos\phi + \hat{\mathbf{e}}_2 \sin\phi)}{\sqrt{1+u_{s'}^2-2\mu' u_{s'}}}.$$

It follows that the integral over an azimuthal angle acts only on the diads, yielding

$$\int_0^{2\pi} \frac{d\phi}{2\pi} (\mathbf{I}-\hat{\mathbf{w}}\hat{\mathbf{w}}) = \left(1 - \frac{1}{2} \frac{1-\mu'^2}{(u_{s'}^2+1-2\mu' u_{s'})}\right)(\mathbf{I}-\hat{\mathbf{e}}_\mathbf{r}\hat{\mathbf{e}}_\mathbf{r}) + \left(\frac{1-\mu'^2}{(u_{s'}^2+1-2\mu' u_{s'})}\right)\hat{\mathbf{e}}_\mathbf{r}\hat{\mathbf{e}}_\mathbf{r}.$$

Because there is only one preferred direction in velocity space ($\hat{\mathbf{e}}_\mathbf{r}$), we are able to write $\langle \Delta \mathbf{v}\, \Delta \mathbf{v}\rangle_s$ in the form

$$\langle \Delta \mathbf{v}\, \Delta \mathbf{v}\rangle_{ss'} = \tfrac{1}{2}\langle \Delta v_\perp^2\rangle_{ss'}(\mathbf{I}-\hat{\mathbf{e}}_\mathbf{r}\hat{\mathbf{e}}_\mathbf{r}) + \langle \Delta v_\parallel^2\rangle_{ss'}\hat{\mathbf{e}}_\mathbf{r}\hat{\mathbf{e}}_\mathbf{r},$$

where the rate of increase in the transverse velocity dispersion is given by

$$\langle \Delta v_\perp^2\rangle_{ss'} = 2\nu_0^{s/s'} v_s^2 \frac{v_s}{v_{s'}} \int_{-1}^{1} d\mu' \frac{H(|\mu'|-\mu_0)}{2(1-\mu_0)} \times \left[\left(\frac{1}{\sqrt{u_{s'}^2+1-2\mu' u_{s'}}} - \frac{1}{2}\frac{1-\mu'^2}{(u_{s'}^2+1-2\mu' u_{s'})^{3/2}}\right)\right],$$

and the rate of increase in the longitudinal velocity dispersion is given by

$$\langle \Delta v_\parallel^2\rangle_{ss'} = \nu_0^{s/s'} v_s^2 \frac{v_s}{v_{s'}} \int_{-1}^{1} d\mu' \frac{H(|\mu'|-\mu_0)}{2(1-\mu_0)} \times \left(\frac{1-\mu'^2}{(u_{s'}^2+1-2\mu' u_{s'})^{3/2}}\right).$$

Two integrals remain to be evaluated,

$$I_1(\mu,u) = \frac{1}{2(1-\mu_0)} \int^{\mu} \frac{d\mu'}{\sqrt{1+u^2-2\mu' u}} = -\frac{1}{u}\frac{\sqrt{1+u^2-2\mu u}}{2(1-\mu_0)}$$

and

$$I_2(\mu,u) = \frac{1}{2(1-\mu_0)} \int^{\mu} \frac{1-\mu'^2}{(1+u^2-2\mu' u)^{3/2}} d\mu' = \frac{1-\mu^2}{u}\frac{(1+u^2-2\mu u)^{-1/2}}{2(1-\mu_0)} - \frac{2\mu}{u^2}\frac{(1+u^2-2\mu u)^{1/2}}{2(1-\mu_0)} - \frac{2}{3u^3}\frac{(1+u^2-2\mu u)^{3/2}}{2(1-\mu_0)}.$$

Combining these results, we obtain the rate of increase in the transverse velocity dispersion,

$$\langle \Delta v_\perp^2 \rangle_s = 2 \sum_{s'} \nu_0^{s/s'} v_s^2 \frac{v_s}{v_{s'}} I_\perp(\mu_0, u_{s'}),$$

and the rate of increase in the longitudinal velocity dispersion,

$$\langle \Delta v_\parallel^2 \rangle_s = \sum_{s'} \nu_0^{s/s'} v_s^2 \frac{v_s}{v_{s'}} I_\parallel(\mu_0, u_{s'}),$$

where

$$I_\perp(\mu_0,u) \equiv \left(\frac{I_1(1,u) - I_1(\mu_0,u) + I_1(-\mu_0,u) - I_1(-1,u)}{2(1-\mu_0)} - \frac{I_2(1,u) - I_2(\mu_0,u) + I_2(-\mu_0,u) - I_2(-1,u)}{4(1-\mu_0)} \right)$$

and

$$I_\parallel(\mu_0,u) \equiv \frac{I_2(1,u) - I_2(\mu_0,u) + I_2(-\mu_0,u) - I_2(-1,u)}{2(1-\mu_0)}.$$

For $\mu_0 \approx 1$ (corresponding to radial locations in the bulk plasma, where $r \gg r_0$), the IEC distribution function corresponds to two counterstreaming beams. We can remove the contribution of collisions between comoving particles from the collision integrals, $I_\perp$ and $I_\parallel$, by replacing the upper limit of 1 in the integrals I_1 and I_2 with $\mu_c < 1$. This results in the modified collision integrals,

$$I'_\perp(\mu_0,u|\mu_c) \equiv \left(\frac{I_1(\mu_c,u) - I_1(\mu_0,u) + I_1(-\mu_0,u) - I_1(-1,u)}{2(1-\mu_0)} - \frac{I_2(\mu_c,u) - I_2(\mu_0,u) + I_2(-\mu_0,u) - I_2(-1,u)}{4(1-\mu_0)} \right)$$

and

$$I'_\parallel(\mu_0,u|\mu_c) \equiv \frac{I_2(\mu_c,u) - I_2(\mu_0,u) + I_2(-\mu_0,u) - I_2(-1,u)}{2(1-\mu_0)}.$$

The angular width of the counterstreaming beams, μ_0, increases toward the plasma core ($r \lesssim r_0$). Hence, the proper choice of μ_c involves a tradeoff between eliminating the effects of collisions between comoving particles over most of the plasma bulk, while minimizing the effect of the cutoff on the collision operator near the plasma core, where the ion distribution function becomes isotropic, and the ansatz of counterstreaming beams breaks down. Our experience indicates that $\mu_c \approx 0.95$ provides an adequate compromise.

Finally, we note that

$$\lim_{\mu_0 \to 1} [I'_\perp(\mu_0,u)] = \frac{1}{2} \frac{1}{|u_{s'}+1|}$$

and

$$\lim_{\mu_0 \to 1} [I'_\parallel(\mu_0,u)] \approx \frac{1}{2} \frac{1-\mu_0}{|u_{s'}+1|^3} \to 0.$$

[1] A. Sakharov, *Memoirs* (Random House, New York, 1992), p. 139.
[2] R. L. Hirsch, J. Appl. Phys. **38**, 4522 (1967).
[3] O. A. Lavrent'ev, Uk. Fiz. Zh. **8**, 440 (1963).
[4] O. A. Lavrent'ev, *Investigations of an Electromagnetic Trap*, Magnitnye Lovushki Vypusk (Naukova Dumka, Kiev, 1968), p. 77 [for an English translation, see Atomic Energy Commission Report No. AEC-TR-7002 (Rev)].
[5] O. A. Lavrent'ev, Ann. NY Acad. Sci. **251**, 152 (1975).
[6] T. J. Dolan, Plasma Phys. Controlled Fusion **36**, 1539 (1994).
[7] D. C. Barnes, R. A. Nebel, and L. Turner, Phys. Fluids B **5**, 3651 (1993).
[8] R. W. Bussard, "Method and apparatus for controlling charged particles," U.S. Patent No. 4,826,646 (2 May 1989).
[9] R. W. Bussard, Fusion Technol. **19**, 273 (1991).
[10] N. A. Krall, Fusion Technol. **22**, 42 (1992).
[11] M. Rosenberg and N. A. Krall, Phys. Fluids B **4**, 1788 (1992).
[12] H. S. Bosch and G. M. Hale, Nucl. Fusion **32**, 611 (1992).
[13] G. H. Miley, J. Nadler, T. Hochberg, Y. Gu, O. Barnouin, and J. Lovberg, Fusion Technol. **19**, 840 (1991).
[14] J. F. Santarius, K. H. Simmons, and G. A. Emmert, Bull. Am. Phys. Soc. **39**, 1740 (1994).
[15] G. H. Miley and H. Towner, *Conference on Nuclear Cross Sections and Technology*, Washington, DC (National Bureau of Standards, Washington, DC, 1975), Vol. 2, p. 716, CONF-750303NBS Special Publication 425.
[16] D. L. Book, *NRL Plasma Formulary*, Naval Research Laboratory Publication No. 0084-4040 (U.S. Department of the Navy, Naval Research Laboratory, Washington, DC, 1986), p. 31.
[17] The 2-D analog of this calculation applies to systems with rotational symmetry like the MIGMA. Here ion focusing results from the constancy of the canonical angular momentum while the ion density falls with radius as $1/r$. Hence, off-axis collisions will again cause a loss of the ion focus on the (volume-averaged) ion collisional time scale.
[18] T. J. Dolan, Fusion Technol. **24**, 128 (1993).
[19] See e.g., C. W. Barnes, Ann. NY Acad. Sci. **251**, 370 (1975); S. K. Wong and N. A. Krall, Phys. Fluids B **5**, 1706 (1993).
[20] V. I. Kogan, in *Plasma Physics and the Problem of Controlled Thermonuclear Reactions* (Pergamon, New York, 1961), Vol. 1, p. 153.
[21] V. P. Pastukhov, Nucl. Fusion **14**, 3 (1974).
[22] R. H. Cohen M. E. Rensink, A. A. Mirin, and T. A. Cutler, Nucl. Fusion **18**, 1229 (1978).
[23] See, e.g., D. E. Baldwin and B. G. Logan, Phys. Rev. Lett. **43**, 1318 (1979); X. Z. Li and G. A. Emmert, Nucl. Fusion **24**, 359 (1984); R. S. Devoto, L. L. LoDestro, and A. A. Mirin, Nucl. Fusion **27**, 255 (1987).
[24] T. H. Rider, "Fundamental limitations on plasma fusion systems not in thermodynamic equilibrium," Ph.D. thesis, Massachusetts Institute of Technology, 1995; submitted to Phys. Rev. Lett. (August, 1995).
[25] A lower limit on a/r_0 is required within our model because the upper limit on the fusion gain goes to $Q_{DT} \lesssim \infty$ if we abandon the IEC concept and let $a/r_0 \to 1$. This unphysical result follows because we have neglected the power required to maintain the ion-confining potential.
[26] D. C. Barnes, R. A. Nebel, and T. N. Tiouririne, Bull. Am. Phys. Soc. **39**, 1739 (1994).
[27] M. N. Rosenbluth, W. M. MacDonald, and D. L. Judd, Phys. Rev. **107**, 1 (1957). See, especially, Eqs. (18) and (19).